Plasma Low-Pressure Nonsteady Diffusion Fluid Model for Pulsed Plasma Recovery

Yi Li, Bocong Zheng, and M. K. Lei

***Abstract*—In order to describe the diffusion behavior of low-pressure plasma, the low-pressure nonsteady diffusion fluid model is built using the equations of ion continuity and ion motion, Boltzmann's relationship of the electron, and variable mobility of the ion. The plasma recovery process in pulsed plasma is described by this model from the viewpoint of diffusion, which is the basic physical mechanism causing recovery. The fluid model is verified to be accurate compared with the particle-in-cell method. The characteristics of multipulse sheath dynamics are studied using this model for inner surface modification of a tube by the plasma-based ion implantation (PBII). Compared with the no-diffusion case, the sheath expansion during pulse-on time is accelerated, and the sheath is thicker when considering the plasma diffusion. During pulse-off time, the plasma recovery behavior of the ion-depleted region is obtained. For a shorter pulse-off time, the plasma cannot recover to its initial state. The maximum of the ion-implantation current can be strongly decreased due to the incomplete plasma recovery, but the average ion-implantation current is improved and achieves its maximum when the duty cycle is 0.8. All these results can provide beneficial theoretical guidance for the parameter optimization in the PBII.**

***Index Terms*—Fluid model, plasma-based ion implantation (PBII), plasma diffusion, plasma recovery.**

I. Introduction

PLASMA-BASED ion implantation (PBII) is a new type of technique for surface modification, and a large number of experiments [1]–[4] have proved that PBII has a significant effect in improving the surface hardness [5], corrosion resistance [6], and wear property of materials [7]. In the PBII, the ions are accelerated by a high pulsed negative voltage and implanted into a target [8]. As the phenomenon is important for PBII applications, it has been investigated by analytical theories and computer simulations in the past [9]–[13]. However, these existing models only consider the effect of a single voltage pulse, under the assumption that the ions have enough time between pulses to flow back into the ion-depleted region, where the ions are implanted into the target during pulse-on time. However, the off time between pulses is generally not long enough for complete plasma recovery, and the low plasma density near the target must affect the sheath expansion and the ion-implantation current in the next pulse-on time. Tian and Chu [14] proposed that the process efficiency of PBII is mostly affected by the experiment on the pulse repetition rate, which demonstrated that the effect of pulsed plasma recovery on the pulsed plasma process is worth studying. There are several theoretical and numerical studies on the plasma recovery process after pulse-on time as well. Wood [15] used the particle-in-cell (PIC) method to exemplify the effects of incomplete plasma recovery. En and Cheung [16] incorporated this PIC method into their circuit simulator model and suggested that the sheath would collapse during the pulse fall time with the Bohm velocity. Daube *et al.* [17] investigated the relaxation phenomenon of the sheath and presheath with fluid and PIC methods. All the aforementioned work did not include the quantitative results about the effect of the recovery process on the ion-implantation parameters. Briehl and Urbassek [18] studied the effects of pulse frequency and duty cycle on the ion-implantation current with the hybrid PIC simulation code. The PIC method needs a lot of calculation, particularly when the collision is considered, whereas the simulation results of the PIC and fluid methods are almost the same when the self-consistent electromagnetism field of the ion is ignored in the PIC method to simplify the calculation [19]–[21]. Chung *et al.* [22], [23] proposed a fluid model to study plasma recovery, but the plasma ambipolar diffusion, which is the main reason causing plasma recovery, was ignored in the PBII process.

In this paper, adopting the low-pressure steady ion mobility proposed by Lieberman and Lichtenberg [24], the low-pressure nonsteady diffusion fluid model is built using the equations of ion continuity and ion motion, as well as Boltzmann's relationship of the electron, and the plasma recovery process in pulsed plasma is described by this model from the viewpoint of diffusion, which is the basic physical mechanism causing recovery. It is verified to be accurate compared with the PIC method. The characteristics of multipulse sheath dynamics are studied using the fluid model for inner surface modification of a tube by PBII, and some details, such as the timescale of plasma recovery, the variation of ion density and velocity with time, etc., are obtained, which can provide beneficial theoretical guidance for the parameter optimization in the PBII process.

II. Plasma Low-Pressure Nonsteady Diffusion Fluid Model

The processing pressure is low in the PBII process and less than 0.13 Pa generally. At low pressure, the effective ion

Manuscript received August 21, 2012; revised October 18, 2012; accepted November 22, 2012. Date of publication December 20, 2012; date of current version January 4, 2013. This work was supported in part by the National Science Foundation of China under Grant 50725519 and in part by the Scientific Research Foundation for Teachers of Liaoning University of Technology.

Y. Li is with the Surface Engineering Laboratory, School of Materials Science and Engineering, Dalian University of Technology, Dalian 116024, China, and also with the School of Science, Liaoning University of Technology, Jinzhou 121001, China.

B. Zheng and M. K. Lei are with the Surface Engineering Laboratory, School of Materials Science and Engineering, Dalian University of Technology, Dalian 116024, China (e-mail: surfeng@dlut.edu.cn).

Digital Object Identifier 10.1109/TPS.2012.2231704

velocity for collision of ions with neutrals is the ion drift velocity $|\mathbf{v}_i|$ rather than the ion thermal velocity v_t, and $|\mathbf{v}_i|$ is much larger than v_t over most of the discharge region. Based on the variable mobility [24], the plasma nonsteady diffusion is supposed to be the quasi-steady state at any time, and the ion mobility μ_i is still

$$\mu_i = \frac{2q}{\pi M_i \gamma} \tag{1}$$

where q is the ion charge, M_i is the mass of the ion, $\gamma = |\mathbf{v}_i|/\lambda_i$ is the ion–neutral collision rate, $\lambda_i = 1/(n_g \sigma_m)$ is the ion mean-free path, n_g is the neutral gas density, and σ_m is the momentum transfer cross section. The ion drift velocity $\mathbf{v}_i$ is written as

$$\mathbf{v}_i = \mu_i E. \tag{2}$$

The electron density is governed by Boltzmann's distribution $n_e = n_i \exp(\phi/T_e)$, where n_i is the plasma density, ϕ is the potential, and T_e is the electronic temperature (in electronvolts). The plasma is assumed to be quasi-neutral in the diffusion process, that is, $n_e \approx n_i$, and the electric field E is obtained as

$$E = -T_e \frac{\nabla n_i}{n_i}. \tag{3}$$

The ion flux Γ is shown as

$$\Gamma = n_i \mathbf{v}_i = \frac{-2qT_e}{\pi M_i \gamma} \nabla n_i. \tag{4}$$

Substituting (4) into the ion continuity equation

$$\frac{\partial n_i}{\partial t} + \nabla \cdot \Gamma = 0. \tag{5}$$

Then, (5) becomes

$$\frac{\partial n_i}{\partial t} - \frac{2qT_e}{\pi M_i} \nabla \cdot \left(\frac{1}{\gamma} \nabla n_i \right) = 0. \tag{6}$$

For low-temperature plasma, the ions can be assumed to be cold, and their velocity is determined by the ion motion equation

$$M_i n_i \left[\frac{\partial \mathbf{v}_i}{\partial t} + \mathbf{v}_i \cdot \nabla \mathbf{v}_i \right] = q n_i E - n_i F_c \tag{7}$$

where t is time, and F_c is the collision drag force, which can be written as [25]

$$F_c = \frac{\pi}{2} M_i \gamma \mathbf{v}_i. \tag{8}$$

Substituting (3) and (7) into the ion motion (6)

$$\frac{\partial \mathbf{v}_i}{\partial t} = -\mathbf{v}_i \cdot \nabla \mathbf{v}_i - \frac{qT_e}{M_i n_i} \nabla n_i - \frac{\pi}{2} \gamma \mathbf{v}_i. \tag{9}$$

The diffusion behavior of low-pressure plasma can be described by solving the nonlinear equations (6) and (9).

III. Accuracy of the Model

In order to verify the accuracy of the low-pressure nonsteady diffusion fluid model, the case of PIC in Wood's work [15] is calculated by the fluid model under the same parameters and conditions. Wood's work studied a planar target PBII process: the plasma is a molecular nitrogen plasma of spatially constant density $n_0 = 4 \times 10^{14}$ ions/m^3, the electron temperature T_e is 1 eV, the steady value of the trapeziform pulse voltage is -50 kV, and both the rising and falling times are 1.0 μs. The pulse-on and pulse-off times are 10 and 20 μs, respectively. Because the collision is not considered in Wood's work, the ion sheath dynamics during pulse-on time is simulated using the collisionless fluid model in this paper. The low-pressure nonsteady diffusion fluid model adopts the mobility that depends on the ion–neutral collision rate, and the collision cannot be ignored. For 1-D planar geometry, the collisionless fluid model that describes the sheath dynamics during pulse-on time and the low-pressure nonsteady diffusion fluid model that describes the plasma recovery process during pulse-off time are shown as

$$\begin{aligned}
&\frac{\partial n_i}{\partial t} + \frac{\partial}{\partial x}(n_i v_i) = 0 \\
&\frac{\partial v_i}{\partial t} + v_i \frac{\partial v_i}{\partial x} = -\frac{e}{M_i} \frac{\partial \phi}{\partial x} \\
&\frac{\partial^2 \phi}{\partial x^2} = -\frac{e}{\varepsilon_0} \left(n_i - n_0 \exp\left(\frac{\phi}{T_e} \right) \right) \qquad (10) \\
&\frac{\partial n_i}{\partial t} + \frac{\partial}{\partial x} \left(\frac{2e\lambda_i T_e}{\pi M_i v_i} \frac{dn_i}{dx} \right) = 0 \\
&\frac{\partial v_i}{\partial t} = -v_i \frac{\partial v_i}{\partial x} - \frac{eT_e}{M_i n_i} \frac{dn_i}{dx} + \frac{\pi}{2} \frac{v_i^2}{\lambda_i} \qquad (11)
\end{aligned}$$

where e is the electron charge, and ε_0 is the permittivity of free space. The following formulas are used to fit the experimental data from Phelps [26] for the momentum transfer cross section σ_m:

$$\begin{cases} \sigma_m = \left(56.46 + \frac{38.34}{\sqrt{\varepsilon}} \right) \times 10^{-20}\ \mathrm{m}^2, & \varepsilon \geq 10^{-4}\ \mathrm{eV} \\ \sigma_m = 3.89 \times 10^{-17}\ \mathrm{m}^2, & \varepsilon < 10^{-4}\ \mathrm{eV} \end{cases} \tag{12}$$

where $\varepsilon = v_i^2 M_i/(2e)$ is the laboratory energy of N_2^+ (in electronvolts). During the calculation, the space and time steps are taken as 0.08 cm and 0.05 ns, respectively. The position where ions have the Bohm velocity is set as the sheath boundary, and the sheath is assumed to be immediately vanished after the end of the pulse; during pulse-off time, the potential of the target is zero.

Fig. 1 shows the comparison of ion-implantation current variation with time at the target for three pulses by PIC and fluid models for a planar target modification by PBII. The calculation result of Wood's PIC work [see Fig. 1(a)] and the calculation results at the processing pressures of 0.133 and 0.030 Pa by the fluid model [see Fig. 1(b)] indicated that the ion currents of the two methods are almost the same for the first pulse, but for the latter two pulses, the ion current at 0.030 Pa is closer to

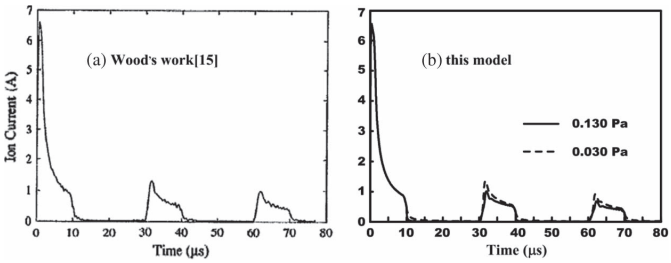

Fig. 1. Time dependence of the ion-implantation current for the (a) PIC and (b) fluid models for a planar target modification by PBII.

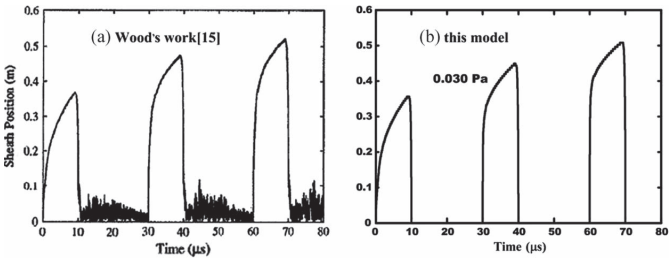

Fig. 2. Time dependence of the sheath position for the (a) PIC and (b) fluid models for a planar target modification by PBII.

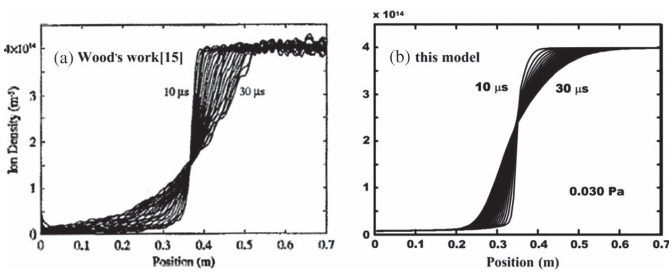

Fig. 3. Time dependence of the ion density distribution at 1-μs intervals in 20 μs between pulses. (a) PIC and (b) fluid models for a planar target modification by PBII.

the PIC case, and at 0.133 Pa, it is slightly smaller. It is shown that the maximal ion-implantation current is 1.36 A/m^2 in the second pulse for the PIC case, and for the fluid model, the maximal ion-implantation currents are 1.01 and 1.35 A/m^2 at 0.133 and 0.030 Pa, respectively, due to the collisional effects. At higher pressure, the collision of ions with neutrals resists the ion drift and decelerates the plasma diffusion process, the ions diffusing into the ion-depleted region in the pulse-off time are reduced, and the ion current in the latter two pulses is slightly smaller compared with the PIC case when not considering collision. When the pressure is decreased, the collision is weakened, and the result of the fluid model is very close to that of the PIC case. Figs. 2 and 3 show the comparison of sheath position and ion density distribution variation with time by PIC and fluid models under a processing pressure of 0.030 Pa, respectively. From the comparison, it is shown that the results of the PIC case and the fluid model are well consistent with each other. Therefore, the aforementioned results can verify that the low-pressure nonsteady diffusion fluid model is reasonable and accurate to describe the diffusion behavior of low-pressure plasma.

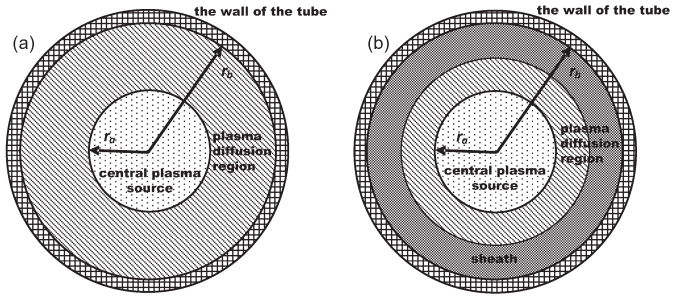

Fig. 4. Schematic of the low-pressure nonsteady diffusion fluid model with a cylindrical coordinate for inner surface modification of a tube by PBII. (a) Tube without the pulse voltage. (b) Tube with the pulse voltage (r_a, plasma source radius; r_b, radius of the tube component).

IV. Low-Pressure Nonsteady Diffusion Fluid Model for Pulsed Plasma Recovery

To study the pulsed plasma recovery behavior, an infinite long tube is assumed to be the research object for the inner surface modification process by PBII [27]. Fig. 4 shows the schematic of the low-pressure nonsteady diffusion fluid model with a cylindrical coordinate for inner surface modification of a tube by PBII. Before the voltage pulse is applied onto the tube, the plasma with a uniform density is continually produced from the central plasma source, the plasma will diffuse from the source to the inner surface of the tube and finally achieves a steady state, namely, there is a steady density distribution between the plasma source and the inner surface of the tube [see Fig. 4(a)]. When a voltage pulse is applied, the plasma diffusion region in Fig. 4(a) is divided into two layers: the region near the inner surface of the tube is the ion matrix sheath, and the other region is still the plasma diffusion region [see Fig. 4(b)].

A. Process Conditions, Model, and Simulation

The plasma with only one type of ion, i.e., N_2^+, is assumed, and the following typical parameters are applied: the central plasma source density n_0 is 1×10^{16} ions/m^3, and the electron temperature T_e is 2 eV. The processing pressure is 0.1 Pa, and the corresponding neutral gas density n_g is 2.65×10^{19} ions/m^3. The steady value of the pulse voltage is -2 kV, the rising and falling times are both 1.0 μs, and the pulse-on time is 10 μs. For 1-D cylindrical coordinates, the equations of the sheath collisional model that describes the sheath dynamics during pulse-on time and the low-pressure nonsteady diffusion fluid model that describes the pulsed plasma recovery process during pulse-off time are shown as follows:

$$\frac{\partial n_i}{\partial t} + \frac{1}{r}\frac{\partial}{\partial r}(r n_i v_i) = 0$$
$$\frac{\partial v_i}{\partial t} + v_i \frac{\partial v_i}{\partial r} = -\frac{e}{M_i}\frac{\partial \phi}{\partial r} - \frac{\pi}{2}\gamma v_i$$
$$\frac{1}{r}\frac{\partial}{\partial r} r \frac{\partial \phi}{\partial r} = -\frac{e}{\varepsilon_0}\left(n_i - n_0 \exp\left(\frac{\phi}{T_e}\right)\right) \quad (13)$$
$$\frac{\partial n_i}{\partial t} - \frac{2eT_e}{\pi n_g M_i r}\frac{\partial}{\partial r}\left(\frac{r}{\sigma_m v_i}\frac{\partial n_i}{\partial r}\right) = 0$$
$$\frac{\partial v_i}{\partial t} = -v_i \frac{\partial v_i}{\partial r} - \frac{eT_e}{M_i n_i}\frac{\partial n_i}{\partial r} - \frac{\pi}{2} n_g \sigma_m v_i^2. \quad (14)$$

The central plasma source can provide the plasma with density n_0 continuously [27], and the ion thermal velocity in the source can be ignored compared with the ion drift velocity in the plasma diffusion region and the sheath; thus, the boundary conditions at the plasma source radius r_a are

$$\begin{aligned} n_i|_{r=r_a} &= n_0 \\ v_i|_{r=r_a} &= 0. \end{aligned} \tag{15}$$

After the end of the pulse, the electrons flood in the high-voltage sheath almost immediately, the net charge that produces the electric field in the sheath is neutralized, the electric field is vanished, and the ions in the sheath are not further accelerated toward the wall. When all the high-energy ions reached the wall, a floating sheath will be formed by the floating potential on the inner surface of the tube; thus, the ion drift velocity is $v_w = (-2e\phi_w/M_i)^{1/2}$ at the wall when the energy loss is ignored. The floating voltage is

$$\phi_w = -T_e \ln\left[\left(\frac{M_i}{2\pi M_e}\right)^{\frac{1}{2}}\right]. \tag{16}$$

Assuming that the floating sheath exists when the ion velocity is less than v_w, the boundary condition of the ion velocity on the inner wall is

$$\begin{aligned} \left.\frac{\partial v_i}{\partial r}\right|_{r=r_b} &= 0 \qquad & v_i|_{r=r_b} &\geq v_w \\ v_i|_{r=r_b} &= v_B \qquad & v_i|_{r=r_b} &< v_w. \end{aligned} \tag{17}$$

The relationship between v_i and $\partial n_i/\partial r$ is obtained by (2) and (3), and the boundary condition of the ion density on the wall is

$$\begin{aligned} \left.\frac{\partial n_i}{\partial r}\right|_{r=r_b} &= 0 \qquad & v_i|_{r=r_b} &\geq v_w \\ \left.\frac{\partial n_i}{\partial r}\right|_{r=r_b} &= -\frac{\pi n_i}{2\lambda_i} \qquad & v_i|_{r=r_b} &< v_w. \end{aligned} \tag{18}$$

With the aforementioned boundary conditions, (13) and (14) are solved with a finite-difference method, and the pulsed plasma recovery during pulse-off time is studied. During the calculation, the space and time steps are taken as 0.01 cm and 0.02 ns, respectively.

B. Results and Discussion

The initial steady ion density and velocity distributions are obtained by solving (14). The ion density can be normalized by the central plasma source density n_0 as $N = n_i/n_0$, and the diffusion process is assumed to be steady when the change of the normalized ion density between the central plasma source and the inner surface of the tube in 1 μs is less than 10^{-4}. Adopting the steady state as the initial condition, the sheath expansion in pulse-on time $t_{\rm on}$ of 10.0 μs and the recovery behavior of plasma in pulse-off time $t_{\rm off}$ of 20.0 μs are studied.

The plasma diffusion during sheath expansion is considered in the low-pressure nonsteady diffusion fluid model, and the no-plasma-diffusion case is also calculated as a comparison. The plasma density outside the sheath remains unchanged in the no-diffusion case. The position where ions have the Bohm velocity is set as the sheath boundary, and the expansion of the sheath boundary with time is shown in Fig. 5 with and without consideration of the plasma diffusion in the inner surface modification of a tube by the PBII process. The plasma diffusion accelerates the sheath expansion significantly compared with the no-diffusion case, and the sheath thickness when considering the plasma diffusion is 0.31 cm larger at the end of the pulse.

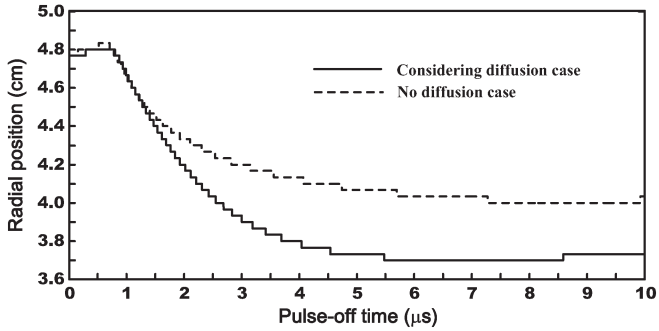

Fig. 5. Evolution of the sheath boundary with pulse-off time in the inner surface modification of a tube by the PBII process.

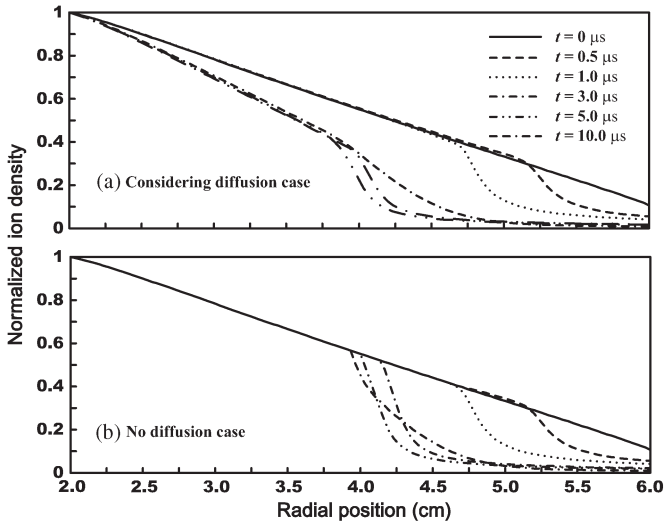

Fig. 6. Distributions of ion density at different times in the inner surface modification of a tube by the PBII process (a) when considering the diffusion case and (b) for the no-diffusion case.

Fig. 6 shows the ion density distribution at different times with and without consideration of the plasma diffusion, which can explain the acceleration effect of sheath expansion by plasma diffusion. With the sheath expansion, the condition of initial steady-state diffusion near the sheath boundary is no longer satisfied, and the ions diffuse into the sheath continuously, which leads to the plasma density gradually decreasing in the plasma diffusion region near the sheath [see Fig. 6(a)]. When the sheath expands more quickly at lower plasma density, the low density caused by the plasma diffusion can accelerate the sheath expansion. For the no-diffusion case, the plasma density in the area outside the sheath remains unchanged because

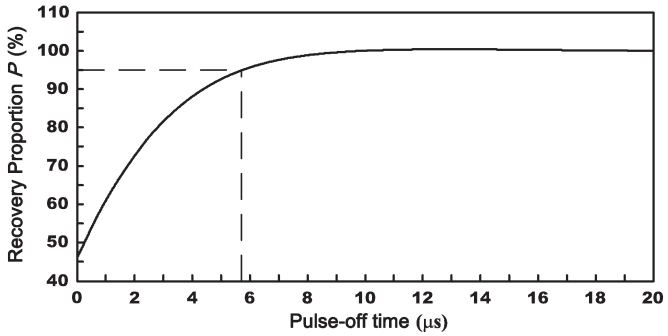

Fig. 7. Variation of the recovery proportion P with pulse-off time in the inner surface modification of a tube by the PBII process.

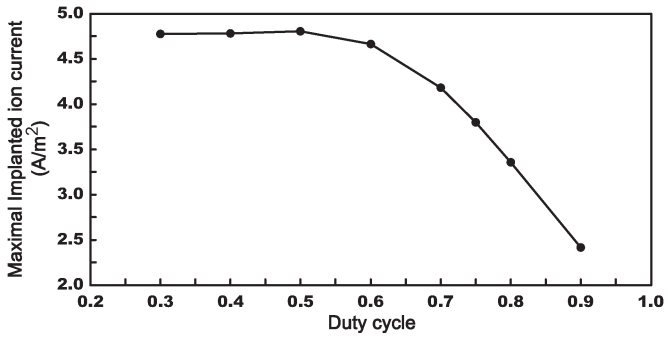

Fig. 8. Variation of the maximal ion-implantation current with the duty cycle in the inner surface modification of a tube by the PBII process.

there is no diffusion; thus, the sheath expansion is slower than the case when considering diffusion [see Fig. 6(b)].

If the ion numbers between the central plasma source and the inner surface of the tube are represented as $N_{\rm In}$ and N_t at the initial steady state and at time t after the end of the pulse, respectively, the plasma recovery ratio can be expressed as $P = N_t/N_{\rm In} \times 100\%$. Fig. 7 shows the variation of the recovery ratio P with time in the inner surface modification of a tube by the PBII process. First, the plasma recovers quickly, P achieves 95% after 5.7 μs, and then the recovery process becomes slower and gradually tends to the steady state. When the plasma density gradient at the beginning of the pulse-off time is much larger than that at the steady state, the electric field is significantly greater, which can be demonstrated by (3), and the diffusion process during pulse-off time is more intense compared with the steady state, which leads to a faster recovery at first. With the plasma density distribution nearing the steady state, the electric field force and the collision drag force being applied on the ions are close to balance, which causes relatively weak plasma diffusion; at this time, the plasma recovery caused by diffusion is very small.

Fig. 8 shows the variation of the maximal ion-implantation current with the duty cycle in the inner surface modification of a tube by the PBII process. With the increasing duty cycle, the maximal current becomes smaller because the incomplete recovery reduces the plasma density near the inner surface at the initial of the pulse-on time.

The ion-implantation dose cannot be scaled only through the maximum of the ion-implantation current in the pulse-on time; thus, the average ion-implantation current is a more

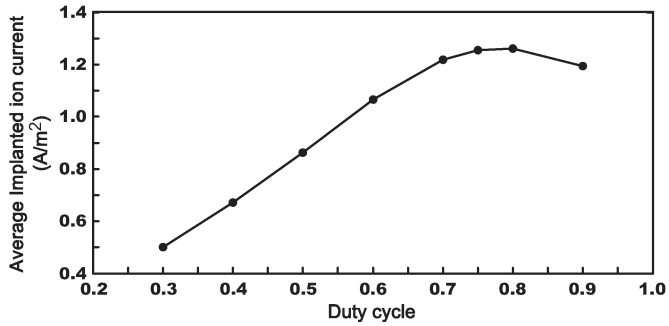

Fig. 9. Variation of the average ion-implantation current with the duty cycle in the inner surface modification of a tube by the PBII process.

appropriate method. During pulse-on time, most of the ions implanted into the target with a high energy accelerated by the high-voltage pulse. In addition, during pulse-off time, most of the ions impact on the wall by v_w, and high-energy ions rarely exist. For an effective modification, the ion-implantation energy needs to be more than a certain value, which is set as 1000 eV here, and the ion-implantation current is achieved by averaging the current in the whole pulse, including pulse-on and pulse-off times. The average current represents the number density of the implanted ions during the whole pulse: the larger the average ion-implantation current, the higher the ion-implantation dose within a period of time. Fig. 9 shows the variation of the average ion-implantation current with the duty cycle in the inner surface modification of a tube by the PBII process. A dramatic improvement in the average ion-implantation current with the increasing duty cycle can be obtained. The maximum value of the average ion-implantation current is 1.26 A/m^2 when the duty cycle is 0.8, but it decreases to 1.19 A/m^2 when the duty cycle is 0.9 and to only 0.5 A/m^2 when the duty cycle is 0.3. Therefore, in order to achieve a larger ion-implantation dose, the duty cycle should have an optimal value.

V. Conclusion

1) The plasma nonsteady diffusion is supposed to be quasi-steady at any time, the ion motion is dominated by the ion mobility, the electron motion is determined by Boltzmann's equilibrium, and the ion flux adopting the variable mobility is applied into the equation of ion continuity. Utilizing the aforementioned assumptions and combined with the ion motion equation, the low-pressure nonsteady diffusion fluid model is built up, and the plasma recovery process in pulsed plasma is described by this model from the viewpoint of diffusion, which is the basic physical mechanism causing recovery.
2) The simulation result of the low-pressure nonsteady diffusion fluid model under 0.030 Pa pressure is very close to Wood's PIC result, which can verify that the plasma low-pressure nonsteady diffusion fluid model is reasonable and accurate to describe the diffusion behavior of low-pressure plasma.
3) The characteristics of multipulse sheath dynamics are studied by the plasma low-pressure nonsteady diffusion fluid model in the PBII process for inner surface modification of a tube. The simulation results demonstrate

that plasma diffusion can accelerate the sheath evolution during pulse-on time. For a shorter pulse-off time, the plasma cannot recover to its initial state. The maximum of the ion-implantation current can be strongly decreased due to the incomplete plasma recovery, but the average ion-implantation current is improved, and in order to obtain the higher ion-implantation dose, the duty cycle should have an optimal value of 0.8.

ACKNOWLEDGMENT

The authors would like to thank Dr. Z. L. Dai, Z. Y. Wang, and Z. P. Zhang for the contributory discussions.

REFERENCES

[1] K. C. Walter, "Nitrogen plasma source ion implantation of aluminum," *J. Vac. Sci. Technol. B, Microelectron. Nanometer Struct.*, vol. 12, no. 2, pp. 945–950, Mar. 1994.

[2] K. C. Walter, J. T. Scheuer, P. C. McIntyre, P. Kodali, N. Yu, and M. Nastasi, "Increased wear resistance of electrodeposited chromium through applications of plasma source ion implantation techniques," *Surf. Coat. Technol.*, vol. 85, no. 1/2, pp. 1–6, Nov. 1996.

[3] W. Wang, J. H. Booske, C. Baum, C. Clothier, N. Zjaba, and L. Zhang, "Modification of bearing steel surface by nitrogen plasma source ion implantation for corrosion protection," *Surf. Coat. Technol.*, vol. 111, no. 1, pp. 97–102, Jan. 1999.

[4] L. Tan, R. A. Dodd, and W. C. Crone, "Corrosion and wear-corrosion behavior of NiTi modified by plasma source ion implantation," *Biomaterials*, vol. 24, no. 22, pp. 3931–3939, Oct. 2003.

[5] G. A. Collins, R. Hutchings, and J. Tendys, "Plasma immersion ion implantation of steels," *Mater. Sci. Eng., A*, vol. 139, pp. 171–178, Jul. 1991.

[6] K. C. Walter, R. A. Dodd, and J. R. Conrad, "Corrosion behavior of nitrogen implanted aluminum," *Nucl. Instrum. Methods Phys. Res. B, Beam Interact. Mater. At.*, vol. 106, no. 1–4, pp. 522–526, Dec. 1995.

[7] X. Qiu, R. A. Dodd, J. R. Conrad, A. Chen, and F. J. Worzala, "Microstructural study of nitrogen-implanted Ti–6Al–4V alloy," *Nucl. Instrum. Methods Phys. Res. B, Beam Interact. Mater. At.*, vol. 59-60, pt. 2, pp. 951–956, Jul. 1991.

[8] J. R. Conrad, J. L. Radtke, R. A. Dodd, F. J. Worzala, and N. C. Tran, "Plasma source ion-implantation technique for surface modification of materials," *J. Appl. Phys.*, vol. 62, no. 11, pp. 4591–4596, Dec. 1987.

[9] J. R. Conrad, "Sheath thickness and potential profiles of ion-matrix sheaths for cylindrical and spherical electrodes," *J. Appl. Phys.*, vol. 62, no. 3, pp. 777–779, Aug. 1987.

[10] G. A. Emmert and M. A. Henry, "Numerical simulation of plasma sheath expansion, with applications to plasma-source ion implantation," *J. Appl. Phys.*, vol. 71, no. 1, pp. 113–117, Jan. 1992.

[11] T. E. Sheridan, "Particle-in-cell simulation of the pulsed sheath in a trench," *IEEE Trans. Plasma Sci.*, vol. 24, no. 1, pp. 57–58, Feb. 1996.

[12] B. Liu, G. L. Zhang, D. J. Cheng, C. Z. Liu, R. He, and S. Z. Yang, "Inner surface coating of TiN by the grid-enhanced plasma source ion implantation technique," *J. Vac. Sci. Technol. A, Vac. Surf. Films*, vol. 19, no. 6, pp. 2958–2962, Nov. 2001.

[13] X. B. Tian, C. Z. Gong, Y. X. Huang, H. F. Jiang, S. Q. Yang, R. K. Y. Fu, and P. K. Chu, "Theoretical investigation of plasma immersion ion implantation of cylindrical bore using hollow cathode plasma discharge," *Surf. Coat. Technol.*, vol. 203, no. 17/18, pp. 2727–2730, Jun. 2009.

[14] X. B. Tian and P. K. Chu, "Modeling of the relationship between implantation parameters and implantation dose during plasma immersion ion implantation," *Phys. Lett. A*, vol. 277, no. 1, pp. 42–46, Nov. 2000.

[15] B. P. Wood, "Displacement current and multiple pulse effects in plasma source ion implantation," *J. Appl. Phys.*, vol. 73, no. 10, pp. 4770–4778, May 1993.

[16] W. En and N. W. Cheung, "Analytical modeling of plasma immersion ion implantation target current using the spice circuit simulator," *J. Vac. Sci. Technol. B, Microelectron. Nanometer Struct.*, vol. 12, no. 2, pp. 833–837, Mar. 1994.

[17] T. Daube, P. Meyer, K. U. Riemann, and H. Schmitz, "Relaxation phenomena in pulsed discharges," *J. Appl. Phys.*, vol. 91, no. 4, pp. 1787–1796, Feb. 2002.

[18] B. Briehl and H. M. Urbassek, "Plasma recovery in plasma immersion ion implantation: Dependence on pulse frequency and duty cycle," *J. Phys. D, Appl. Phys.*, vol. 35, no. 5, pp. 462–467, Mar. 2002.

[19] A. Friedman, S. E. Parker, S. L. Ray, and C. K. Birdsall, "Multi-scale particle-in-cell plasma simulation," *J. Comput. Phys.*, vol. 96, no. 1, pp. 54–70, Sep. 1991.

[20] R. Faehl, B. Devolder, and B. Wood, "Application of particle-in-cell simulation to plasma source ion implantation," *J. Vac. Sci. Technol. B, Microelectron. Nanometer Struct.*, vol. 12, no. 2, pp. 884–888, Mar. 1994.

[21] T. E. Sheridan, "Ion focusing by an expanding, two-dimensional plasma sheath," *Appl. Phys. Lett.*, vol. 68, no. 14, pp. 1918–1920, Apr. 1996.

[22] K. J. Chung, S. W. Jung, J. M. Choe, G. H. Kim, and Y. S. Hwang, "Self-consistent circuit model for plasma source ion implantation," *Rev. Sci. Instrum.*, vol. 79, no. 2, pp. 02C502-1–02C502-5, Feb. 2008.

[23] K. J. Chung, J. M. Choe, G. H. Kim, and Y. S. Hwang, "Dynamic sheath expansion in a non-uniform plasma with ion drift," *Plasma Sources Sci. Technol.*, vol. 20, no. 4, p. 045014, Aug. 2011.

[24] M. A. Lieberman and A. J. Lichtenberg, *Principles of Plasma Discharges and Materials Processing*. Hoboken, NJ: Wiley, 2005, pp. 144–145.

[25] T. E. Sheridan and M. J. Goeckner, "Collisional sheath dynamics," *J. Appl. Phys.*, vol. 77, no. 10, pp. 4967–4972, May 1995.

[26] A. V. Phelps, "Cross sections and swarm coefficients for nitrogen ions and neutrals in N_2 and argon ions and neutrals in Ar for energies from 0.1 eV to 10 keV," *J. Phys. Chem. Ref. Data*, vol. 20, no. 3, pp. 557–573, May 1991.

[27] Y. Li, B. C. Zheng, and M. K. Lei, "Engineering the tube size for an inner surface modification by plasma-based ion implantation," *Vacuum*, vol. 86, no. 9, pp. 1278–1283, Mar. 2012.

Yi Li received the B.S. degree in physics education and the M.S. degree in theoretical physics from Liaoning Normal University, Dalian, China, in 2007. He is currently working toward the Ph.D. degree in the Surface Engineering Laboratory, School of Materials Science and Engineering, Dalian University of Technology, Dalian. His Ph.D. project is focused on the sheath characteristics of plasma-based low-energy ion implantation for inner surface modification.

Since 2002, he has been with Liaoning University of Technology, Dalian.

Bocong Zheng received the B.Eng. degree in material science and engineering from Dalian Maritime University, Dalian, China, in 2009. He is currently working toward the Ph.D. degree in the Surface Engineering Laboratory, School of Materials Science and Engineering, Dalian University of Technology, Dalian.

M. K. Lei was born in Liaoyang, China, in 1963. He received the B.Sc., M.Sc., and Ph.D. degrees from Dalian University of Technology, Dalian, China, in 1984, 1988, and 1997, respectively, all in materials engineering.

He joined the Surface Engineering Laboratory, Department of Materials Engineering, Dalian University of Technology, in 1984. In 1989, he became an Assistant Professor. From 1991 to 1992, he was with the Institute of Thermophysics, Siberian Branch of the Russian Academy of Sciences, Novosibirsk, Russia, as a Visiting Scientist. In 1996, he became an Associate Professor. Since 1998, he has been a Professor and Head of the Surface Engineering Laboratory, Dalian University of Technology. In 2008, he became a Changjiang Program Professor with Dalian University of Technology. His research interests are in plasma surface science and engineering, thin films and coatings, and surface modification by energetic beams.